Zhao, Weixin; Ejaz, Muhammad Farhan; Kilpeläinen, Simo; Jokisalo, Juha; Kosonen, Risto

The potential of local exhaust combined with mixing and displacement ventilation systems to mitigate COVID-19 transmission risks

Published in:
Building and Environment

DOI:
10.1016/j.buildenv.2024.112076

Published: 01/12/2024

Document Version
Publisher's PDF, also known as Version of record

Building and Environment 266 (2024) 112076

Contents lists available at ScienceDirect

Building and Environment

journal homepage: www.elsevier.com/locate/buildenv

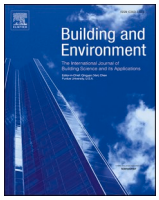

The potential of local exhaust combined with mixing and displacement ventilation systems to mitigate COVID-19 transmission risks

Weixin Zhao [a,*], Muhammad Farhan Ejaz [a], Simo Kilpeläinen [a], Juha Jokisalo [a], Risto Kosonen [a,b]

[a] Department of Mechanical Engineering, Aalto University, Espoo, 02150, Finland
[b] College of Urban Construction, Nanjing Tech University, China

ARTICLE INFO

Keywords:
Airborne transmission
Contaminant removal effectiveness
Dilution ratio
Air distribution
Infection probability

ABSTRACT

The performance of two types of air diffusers, a perforated duct and a low-velocity unit coupled with local exhausts, on airborne transmission and cross-infection was investigated in a meeting room. The effect of air diffusers' locations on airborne transmission was investigated. Six local exhausts were installed above six workstations at 2.0 m height. Respiratory-generated airborne pathogens were simulated using SF_6 in the exhaled air of the manikin acting as an infected person. The SF_6 concentration in the inhaled air of five susceptible persons remained steady with perforated duct located on the ceiling and at 1.7 m height attached to the corridor wall, but fluctuated greatly when perforated duct were located on the floor, although with a much lower concentration level. The perforated duct under the warm window showed the best potential for mitigating airborne transmission. The concentration in the inhaled air was varied with horizontally supplied low-velocity unit, but much steadier with low-velocity unit at 1.7 m attached to the wall. With an adjusted airflow pattern from low-velocity unit, the inhaled concentration was much lower and uniform among the five susceptible persons. The contaminant removal effectiveness (CRE) was 4.3 with perforated duct under a warm window on the floor. With an adjusted airflow pattern from low-velocity unit, the CRE was much more consistent and increased from 2.1 to 3.9 with an airflow rate from 61 l/s to 116 l/s. The infection probability was the lowest with the perforated duct on the floor and adjusted low-velocity unit.

1. Introduction

Effective ventilation plays a crucial role in mitigating airborne cross-infection in the built environment and increasing the ventilation rate can effectively reduce the risk of long-range airborne transmission [1–3]. It has been shown that a higher risk of infection may occur in poorly ventilated spaces because of proper air circulation for reducing the infection probability [4,5]. Recently, it has been clearly proven that airflow distribution methods have a substantial impact on personal exposure to indoor air pollutants [6,7]. The need for occupant-based ventilation systems, such as personalized ventilation instead of central systems, to reduce cross-infections has been highlighted. However, the efficacy of supply air distribution in the occupied zone can vary due to the complex interaction of the expiratory airflow and buoyancy flows [8]. Furthermore, exhaled aerosol droplets from an infected person transmitting to the susceptible persons are affected by the breathing flow, human body boundary layer flow [9], and ventilation flow. It is important to consider various factors beyond just the ventilation volume when evaluating ventilation systems, such as the airflow distribution and direction. A recent study indicated that boosting the ventilation rate might lead to an increased concentration of respiratory pathogens in the inhaled air [10]. The proximity of an infected individual to the air supply unit in displacement ventilation systems can influence the infection risk significantly [11]. This highlights the importance of considering the placement of potential infectors concerning the air supply unit when designing ventilation systems to mitigate infection risks effectively.

Local exhaust systems are extensively utilized in various settings for their effectiveness at removing contaminants. In hospital wards, the local exhaust systems are used to remove infectious contaminants to keep patients and health workers safe [12–14]. A local exhaust system could minimize the number of droplets evaporated in the ward. A personalized exhaust operation can reduce the exposure of a health work more efficiently than an increase of ACH [15]. Moreover, it is critical to

* Corresponding author.
E-mail address: ext-weixin.zhao@aalto.fi (W. Zhao).

https://doi.org/10.1016/j.buildenv.2024.112076
Received 4 July 2024; Received in revised form 2 September 2024; Accepted 8 September 2024
Available online 10 September 2024

maintain the clean air supply to avoid contamination [16] in intensive care units and operating rooms and in industrial workplaces to reduce dust fumes or vapors generated during manufacturing processes [17,18] with a local exhaust. In addition, a local exhaust is used in laboratories to avoid contaminated particles affecting the samples [19], kitchens [20], offices [21], and classrooms [22]. Hence, local exhausts are beneficial for reducing the spread of airborne contaminants and protecting the occupants' health.

A local exhaust is efficient against airborne transmission in densely occupied spaces. Yang et al. [23] found that with a top-personalized exhaust or shoulder-personalized exhaust, the exposure for the healthy person after 30 min was lower than the exposure at 10 min without a personalized exhaust. The combination of physical barriers and personal exhaust ventilation consistently reduced contaminant concentration by 34 %–83 % [21].

Recent studies have proved that the location of the exhaust also has a significant effect on personal exposure to indoor air pollutants [24,25]. Depending on the location of the exhaust, exhaled airborne pathogens can become entrained back into the supply air stream and can eventually spread into the entire room. Through experimental studies conducted for local exhaust ventilation systems, Liu et al. [26] suggested improvements in the capture efficiency by varying the height distance of the exhaust hood, describing its importance in an industrial plant. Furthermore, the height of the local exhaust in an office has a significant effect on energy saving and the indoor environment. Ventilation strategies and furniture layout in the office have a great influence on airflow and pollutant distribution patterns. Improvements in the local exhaust system using jet-like devices inducing using vortex-based airflows have been suggested [27–29] which improve the capture efficiency, and the range of capturing particles given that it is close to the source of contamination. Qian et al. [30] showed that a high-concentration layer of exhaled droplet nuclei existed with displacement ventilation due to thermal stratification. Therefore, if the local exhaust is applied at an appropriate height with displacement ventilation, this layer would not be observed.

In our recent studies [6,31], the performance of local exhaust above the workstation in a meeting room was studied with mixing ventilation (a perforated duct installed on the ceiling) and displacement ventilation (a horizontally supplied low-velocity unit). The airborne transmission and infection risk using the perforated duct and low velocity unit on the floor was quantitatively analyzed. The infection probability for every exposed person was found to be quite uniform with the perforated duct but varied depending on the airflow rate and the relative distance between the low-velocity unit and the exposed person. The local exhaust improved the local air quality significantly, particularly with a low-velocity unit. However, if the location of the perforated duct and low-velocity unit are varied, the airflow pattern and airborne transmission would be different. Studying the impact of varying the location of air diffusers on airborne transmission within a meeting room equipped with a local exhaust system is a novel approach.

The motivation of this study was to optimize the positions of perforated ducts and low-velocity unit to influence airflow patterns and consequently affect the transmission of airborne contaminants in indoor environments. By examining these factors, the study can provide valuable insights into optimizing air distribution systems to enhance indoor air quality and reduce the risk of airborne transmission of pathogens. The novelty of the study is to present the effect of the location of a perforated duct and low-velocity unit together with local exhaust on airborne transmission. In this study, the perforated duct was located at four different locations: in the middle of the ceiling, under a warm window on the floor, below a corridor wall on the floor and attached to the corridor wall at 1.7 m height. With the low-velocity unit, the first setup was located on the floor with a horizontally supplied flow, the second setup was an adjusted air pattern from low-velocity unit with perforated panels, and the third setup was attached to the wall at 1.7 m height.

2. Methods

The experiments were conducted within a full-scale test room, wherein the indoor conditions were controlled. The dimensions of the test room were 5.50 m (length), 3.80 m (width), and 3.60 m (height), resulting in a total floor area of 21 m^2. To maintain a stable environment, the test chamber was situated within a laboratory hall.

2.1. Experimental set-up

2.1.1. Test room

The aim of this experimental setup was to replicate a typical meeting room with a conventional layout. A meeting table accommodating six workstations was positioned in the center of the room, as depicted in Fig. 1. There were six local exhausts installed above the workstations forming a continuous plate over the workstations at a height of 2.0 m with dimensions of 900 mm × 900 mm.

The size of the meeting table was 5.2 m × 0.8 m. Surrounding the table were a breathing thermal manikin, one heated dummy [32], and four heated cylinders. The diameter of the heated cylinder was 0.4 m and the height was 1.1 m including 0.1 m high legs against the vertical air distribution. The dummy and cylinders [33,34] were served as individuals susceptible to thermal plumes, but without the respiratory process. Only the manikin and dummy were equipped with a laptop. Overhead lights were installed in the middle of the workstations, attached to the ceiling panels.

To simulate warm window conditions, one side of the room was equipped with warm radiant panels. These panels were supplied with hot water to achieve the desired surface temperature, replicating summer conditions. Additionally, a heating foil was placed on the floor 0.8 m away from the heated window panel wall to simulate the impact of direct solar radiation. The heat gains used in the test room are summarized in Table 1.

2.1.2. Air distribution methods

This study employed the utilization of mixing and displacement air distribution principles. One of two air diffusers was a perforated duct (Ventiduct VSR duct-diffusers [35]) with a diameter of 200 mm and a total length of 5.5 m, as shown in Fig. 2. Another air diffuser was a low-velocity unit (Zen ZRE – Displacement ventilation unit [36]) measuring 1140 mm × 550 mm.

To study the effect of the location of the air diffuser on the air distribution, the perforated duct (PD) was installed at 4 locations, as shown in Fig. 3: 1) in the middle of the ceiling with a downward airflow (PD-ceiling); 2) under a warm window on the floor with an airflow direction of 45° upwards (PD-warm window); 3) below a corridor wall on the floor with an airflow direction of 45° upwards (PD-corridor wall); 4) attached to the corridor wall at 1.7 m height with av airflow direction of 45° downwards (PD-corridor wall-1.7m).

The low-velocity unit (LV) was installed at 3 locations, as shown in Fig. 4: 1) with horizontally supplied air from a low-velocity unit in the middle of the wall facing the door on the floor (HLV); 2) with airflow pattern adjustment using a low-velocity unit on the floor, combined with two perforated panels angled at 45° and a non-perforated blocker positioned in front of the unit, effectively redirecting the airflow to the side of the meeting table (ALV); 3) attached to the middle of a wall at 1.7 m height and adjusting the direction of the downward airflow using a reflector at a 45° angle (LV-1.7m). The air distribution is modified to resemble adaptive attachment ventilation [37]. The goal of this setup was designed to delivery air above the meeting table while preventing A direct airflow drop onto the floor. The parameters of the designed experimental cases are shown in Table 2. The general exhaust was located on the ceiling in the corner.

2.1.3. Thermal breathing manikin

The thermal breathing manikin (PT Teknik, Hillerød, Denmark)

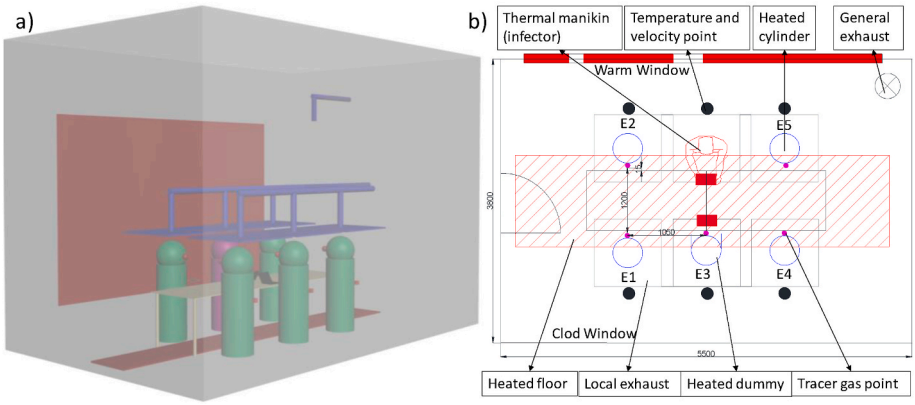

Fig. 1. a) The meeting room set-up and b) top view [mm].

Table 1
The heat gains used in the tests.

Heat flux	W/m^2	67	36
Total heat flux	W	1407	756
Floor area	m^2	21	21
Total heat load	W	1407	756
Manikin	W	80	80
Dummy	W	75	75
4 Cylinder dummies	W	75 × 4 = 300	75 × 4 = 300
2 Lptops	W	2 × 40 = 80	2 × 40 = 80
Light	W	90	90
Window panels	W	317	86
Solar load at floor	W	420	0
Equipment of manikin	W	45	45
Supply airflow rate	l/s	117	63
Air change rate	1/h	5.6	3
Supply air temperature	°C	16	16
Design room air temperature	°C	26	26

utilized in this study consisted of 27 individual body segments that were heated separately, serving as a simulation of an infected individual in a seated position (referred to as the "infector" hereafter). The dimensions of the manikin matched a 1.75 m tall male. The heat power and temperature of each body segment were independently regulated by a computer program. Throughout this experiment, the manikin's surface temperature was meticulously controlled to closely match that of human skin temperature, adhering to the control mode for thermal comfort. Furthermore, the manikin was dressed in attire consisting of a short-haired wig, vest, shirt, trousers, light socks, and light shoes, with a thermal insulation value of 0.5 Clo, imitating the clothing typically worn in an office setting during the summer season.

The nostrils of the manikin were designed as circular openings, each with an area of 44.2 mm^2, while the mouth was shaped as an ellipsoidal opening with an area measuring 113.4 mm^2. Two jets were expelled from the nostrils, angled 45° downward from the horizontal axis.

To replicate natural human breathing, the manikin was connected to an artificial lung. The artificial lung allows realistic simulation of a human like breathing cycle, with timers controlling the air pumps so they can simulate breathing. It consists of an air distribution system, humidifying system and system for maintaining exhaled air temperature. The intended pulmonary ventilation rate was 6.0 l/min [38]. Each breathing cycle consisted of a 2.5-s inhalation phase, followed by a 1.0-s pause, a 2.5-s exhalation phase, and another 1.0-s pause. The exhaled air was mixed with tracer gas from the manikin and heated to a temperature of 35 °C, while also being humidified to 85 %.

2.1.4. *Measured parameters and instrumentation*

In this experimental study, the tracer gas SF_6 was employed to replicate the presence of virus-containing droplet nuclei in the exhaled air of an infected manikin [7]. The tracer gas was introduced continuously into the artificial lung and only released from the nose during the exhalation period. The rest of the tracer gas was removed outside of the room directly. The flow rate of the tracer gas was set to 2 ml/s [39], while the pulmonary ventilation rate of the manikin infector was maintained at 6 l/min. Consequently, the concentration of the tracer gas in the exhaled air of the infected manikin was approximately 20,000 ppm.

Throughout the experiment, the concentration of tracer gas was measured at six different locations by a multi-gas analyzer platform (GASERA one, Turku, Finland) with an accuracy of 0.37 ppm. These locations included inhaled air of five susceptible individuals and general exhaust, as depicted in Fig. 1. The dosing of the tracer gas commenced 1 h after the attainment of steady-state conditions in the indoor environment. The tracer gas measurement in the test room involved two distinct stages. Initially, the concentration of the tracer gas increased following its introduction, and subsequently, it reached a stable value at the general exhaust. All the measurement devices used during the experiments are summarized in Table 3.

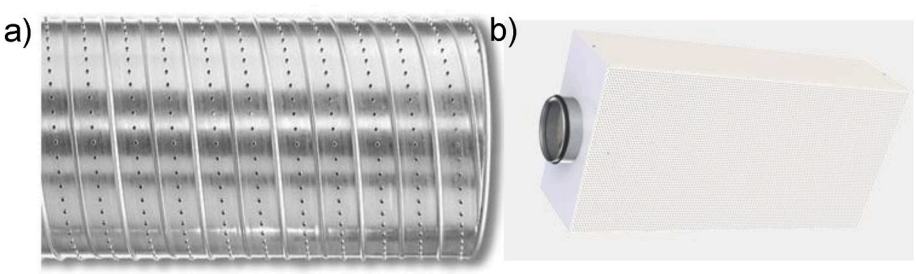

Fig. 2. a) Perforated duct and b) low-velocity unit.

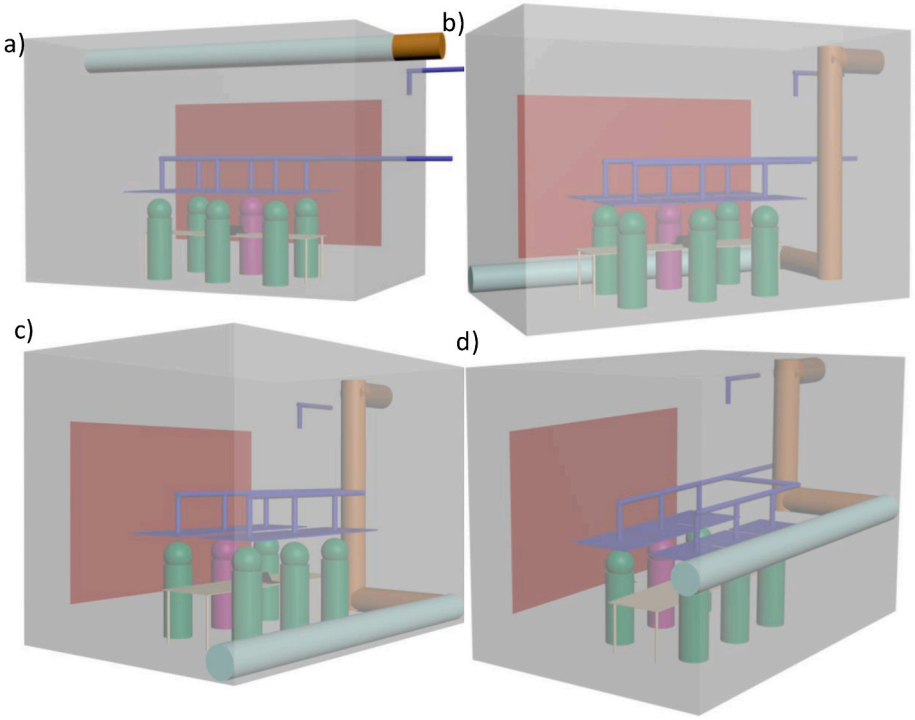

Fig. 3. The location of perforated duct 1) on the middle of ceiling, 2) under the warm window, 3) below the corridor wall and 4) attached to the corridor wall at 1.7 m height.

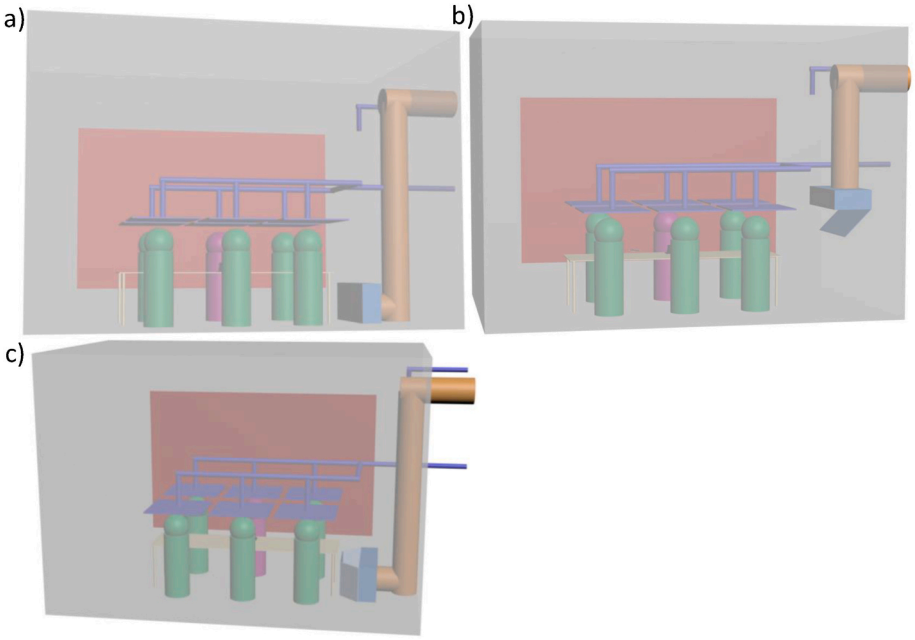

Fig. 4. The location of the low-velocity unit 1) on the floor, 2) modified air direction with perforated panel and 3) attached to the wall at 1.7 m height.

2.2. Experimental conditions and test cases

In this study, the experimental conditions were as follows: the supply air temperature was maintained at 16 °C with an accuracy of ±0.2 °C, while the exhaust air temperature was measured at 26 ± 1 °C according to the heat gain and cooling load balance in Table 1. The relative humidity of the indoor air was not actively controlled and exhibited slight variations ranging from 30 % to 40 % during the experiments.

The supplied airflow was 117 l/s and 63 l/s with a heat gain of 67 W/m^2 and 36 W/m^2, leading to airflow rates of 5.5 l/s per m^2 and 2.9 l/s per m^2, respectively. With an airflow rate of 61 l/s, a total of 30 l/s of exhaust air was extracted through the six local exhausts, with each local exhaust point removing 5 l/s of air. The remaining 31 l/s of air was expelled through the general exhaust. Similarly, with an airflow rate of 116 l/s, exhaust air of 60 l/s was removed from 6 local exhausts (10 l/s per local exhaust), while the rest of the air (56 l/s) was removed by the general exhaust.

Table 2
The test cases with two air diffusers installed at different locations.

Heat flux	Air diffuser	Installed location
67 W/m^2	Perforated duct	PD-Ceiling
		PD-Warm Window
		PD-Corridor Wall
		PD-Corridor Wall-1.7 m
	Low-velocity unit	HLV
		ALV
		LV-1.7 m
36 W/m^2	Perforated duct	PD-Ceiling
		PD-Warm Window
		PD-Corridor Wall
		PD-Corridor Wall-1.7 m
	Low-velocity unit	HLV
		ALV
		LV-1.7 m

Table 3
The measuring instruments.

Variable	Model	Accuracy
Temperature Air velocity Turbulence intensity Draught rate Radiant temperature	Omnidirectional probe 54T33 Draught Probe	Air speed (v): range 0–1.0 m/s Uncertainty: ±2 % or ±0.0 2 m/s on reference velocity Temperature (t): range 0–45 °C ± 0.2 °C on reference temperature 2 Hz
Operative temperature	ComfortSense temperature 54T38	Uncertainty: ±0.3 °C on reference temperature 2 Hz
Pressure difference	IRIS-200 damper	±5 %
Tracer gas concentration	Gasera ONE Multi-gas Sampler and Monitor	Detection limit: 0.37 ppm Repeatability: 0.08 %
Temperature Relative humidity	Tinytag plus 2 TGP- 4500	Air temperature ±0.5 °C, RH ±3 % at 25 °C
Surface temperature	ThermaCAMTM P60 infrared camera	±0.02·Tmeas

2.3. Evaluation indices

The contaminant removal effectiveness (CRE) ε^c, serves as a quantitative measure of the rate at which an airborne contaminant is eliminated from a room [40]. This metric is determined based on various factors including the average concentration of contaminants in the room $< C >$, as well as the contaminant concentration at the supply C_s, and the contaminant concentration at the exhaust C_e, as follows:

$$C_e = \frac{C_e - C_s}{< C > - C_s} \tag{1}$$

To assess the infection risk associated with indoor environments, the Wells-Riley model [41] is commonly employed. This model assumes that the indoor conditions are fully mixed and steady as follows:

$$P = \frac{C}{S} = 1 - e^{-\left(Iqpt/Q\right)} \tag{2}$$

where P is the infection probability, C is the number of new infections, S is the number of susceptible people, I is the number of infectors, q is the quantum generation rate by an infected person (quanta/h), p is the pulmonary ventilation rate (m^3/h), t is the total exposure time (h), and Q is the room ventilation rate (m^3/h).

However, it is important to acknowledge that indoor conditions are not uniform throughout the entire space. Therefore, it is necessary to account for the non-uniformity factor within the probability model. Zhang and Lin [39] proposed a dilution-based evaluation approach to estimate the risk of airborne infection. This approach modifies the Wells-Riley model to accommodate situations where the indoor environment is not fully mixed. The revised Wells-Riley model is as follows:

$$D = \frac{C_{infector}}{C_{susceptible}} \tag{3}$$

$$C_{quantum} = \frac{q}{D * p_{infector}} \tag{4}$$

$$N_{quantum} = \int_0^T p_{susceptible}\, C_{quantum}(t)dt \tag{5}$$

$$P_D = 1 - e^{-N_{quantum}} \tag{6}$$

$$P_D = 1 - e^{-\int_0^T \frac{q * p_{susceptible}}{D(t) * p_{infector}} dt} \tag{7}$$

where $C_{infector}$ and $C_{susceptible}$ are the airborne contaminant concentrations at the infectious point and susceptible position respectively (ppm); $C_{quantum}$ is the airborne quantum concentration at the susceptible position (quanta/m^3); D is the dilution ratio at the susceptible position; $p_{infector}$ is the breathing rate of the infector (m^3/s); $N_{quantum}$ is the inhaled quanta by the susceptible person during the given exposure period; T is the total exposure time (h); P_D is the airborne infection risk for the susceptible person during the given exposure period estimated by the dilution-based estimation method proposed; $p_{susceptible}$ is the breathing rate of the susceptible person (m^3/s).

3. Results

3.1. Airborne transmission

Fig. 5 shows the concentration distribution of the tracer gas with a heat gain of 36 W/m^2 and an airflow rate of 61 l/s with four different installation locations of the perforated duct. The tracer gas concentration was increased with time and reached steady-state conditions after 60 min at the exhaust point. In the steady-state conditions, the average concentration was between 20.1 and 21.6 ppm at the exhaust point.

When the perforated duct was in the middle of the ceiling, under the warm window on the floor and under the corridor wall on the floor, the concentration of the exhaust point was higher than that in the inhaled air of the susceptible persons. This means that the perforated duct can provide cleaner air to the breathing zone than the concentration in fully mixed conditions. The concentration in the inhaled air was much more unaltered for the five susceptible persons when the perforated duct was located on the ceiling and at 1.7 m height. However, it fluctuated a lot when the perforated duct was located on the floor (Fig. 5b and c). The highest SD was 6.1 ppm at position E3 with the perforated duct under the warm window. The average concentration in the inhaled air was 12.7 ppm and 13.6 ppm with the perforated duct located on the floor. The corresponding values were 16.5 ppm and 18.6 ppm with the perforated duct located on the ceiling and at 1.7 m height. Therefore, the tracer gas concentration in the inhaled air was lower but varied when the perforated duct was on the floor. With this installation principle, the air distribution was more like displacement ventilation. The average concentration difference between the five susceptible persons was largest with the perforated duct under the warm window, where 9.0 ppm at position E4 and 16.8 ppm at position E5. The concentration at position E1 and position E2 was lower than other points with the perforated at 1.7 m height.

When the airflow rate increased to 116 l/s with a heat gain of 67 W/m^2 (Fig. 6), the tracer gas concentration increased with time at first and then reached steady-state conditions after 34 min at the exhaust. In the steady-state conditions, the average concentration was between 9.9 and

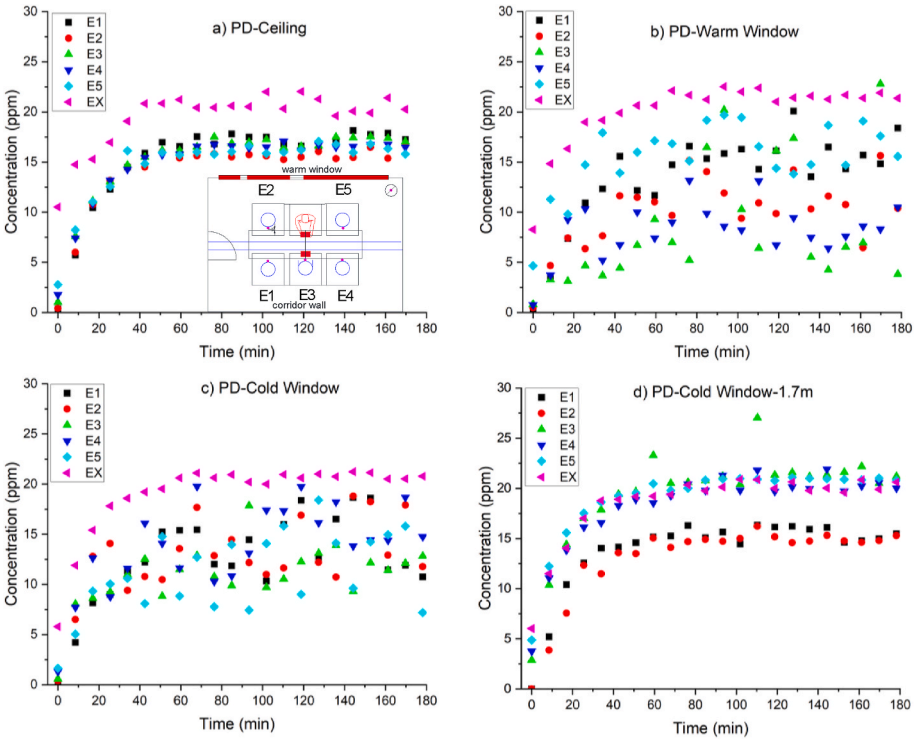

Fig. 5. Tracer gas distribution in the inhaled air of the five susceptible persons and general exhaust as a function of time with the heat gain of 36 W/m^2 and airflow rate of 61 l/s with the perorated duct located a) on the middle of the ceiling, b) under the warm window on the floor, c) below the corridor wall on the floor, and d) attached to the corridor wall at 1.7 m height.

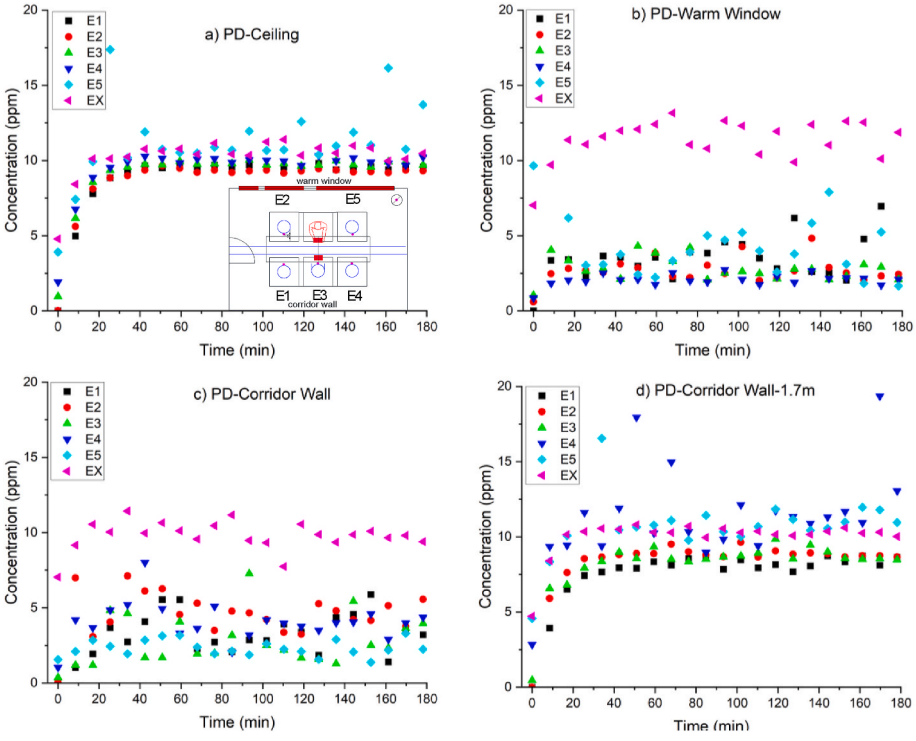

Fig. 6. Tracer gas distribution in the inhaled air of the five susceptible persons and general exhaust point as a function of time with the heat gain of 67 W/m^2 and airflow rate of 116 l/s with the perforated duct located a) on the middle of the ceiling, b) under the warm window on the floor, c) below the corridor wall on the floor, and d) attached to the corridor wall at 1.7 m height.

11.7 ppm when the perforated duct was installed at different locations. Similarly to the case of 61 l/s, the concentration at the exhaust point was much higher than that in the inhaled air when the perforated duct was on the floor (Fig. 6b and c). The average concentration in the inhaled air was 3.1 ppm and 3.5 ppm with the perforated duct located on the floor. The corresponding values were 10.0 ppm and 9.8 ppm with the

perforated duct located on the ceiling and at 1.7 m height. This means the performance of the perforated duct on the floor in terms of mitigating airborne transmission was better with the higher heat gain and higher airflow rate. In general, the maximum and minimum concentration occurred at different susceptible persons with an airflow rate of 61 l/s and 116 l/s. This means the increasing heat gain and airflow rate could adjust the airborne transmission overall in the meeting room.

Fig. 7 shows the concentration distribution of tracer gas with the heat gain of 36 W/m^2 and the airflow rate of 61 l/s with the low-velocity unit (LV). After the tracer gas concentration at the exhaust point reached steady-state conditions, the average concentration was the highest at 23.3 ppm with the low-velocity unit on the floor (Fig. 7 a) and the lowest at 19.3 ppm with the modified air direction from the low-velocity unit (Fig. 7 b). When the low-velocity unit was on the floor and an adjusted airflow pattern from the low-velocity unit, the concentration at the exhaust point was higher than that in the inhaled air of the five susceptible persons. In addition, the concentration in the inhaled air varied in these two settings (Fig. 7a and b). However, the concentration in the inhaled air was much more stable for susceptible persons except position E5 (near the infector and general exhaust) when the low-velocity unit was at 1.7 m height. The average concentration in the inhaled air was 14.8 ppm but reached 30.5 ppm at position E5. With the low-velocity unit at 1.7 m, only a small volume of supply air from the low-velocity unit reached the position E5. Another possible reason for it is under this situation, the contaminant exhaled from the infector (near position E5) transferred to position E5 due to the effect of general exhaust point near position E5. The mean concentration with the adjusted low-velocity unit (10.8 ppm) was lower than the horizontally supplied low-velocity unit (12.0 ppm). This means the horizontally supplied airflow is not a good solution in the meeting room which created eddies at the opposite wall. Therefore, a better solution with low-velocity unit is to direct the flow to reduce the effect of the strong flow. When the low-velocity unit was at 1.7 m height, the average inhaled concentration was the highest (17.9 ppm) and the airflow pattern was more near the mixing ventilation.

When the heat gain was 67 W/m^2 and the airflow rate was 116 l/s with the low-velocity unit, after the tracer gas concentration at the exhaust point reached the steady-state conditions, the average concentration was similar at the exhaust at three settings, at about 11.5 ppm. However, with the adjusted airflow pattern, the concentration at the exhaust was higher than that in the inhaled air (Fig. 8 b). The average inhaled concentration for five susceptible persons was 5.7 ppm and 3.1 ppm with the low-velocity unit on the floor (Fig. 8 a) and with adjusted airflow pattern from the low-velocity unit (Fig. 8 b). However, the value was 11.2 ppm when the low velocity was at 1.7 m height. With the adjusted airflow pattern from the low-velocity unit, the inhaled concentration was much lower and more uniform among the five susceptible persons, which was similar to the case with the lower airflow rate.

However, there were significant variations at position E1 (near the door and far from the diffuser) with the low-velocity unit on the floor. This is because the stronger horizontally supplied air may enhance the airborne transmission following the direction of the air jet. Like the case of 61 l/s, the inhaled concentration at position E5 (near the infector and general exhaust) was much higher and varied with the low-velocity unit at 1.7 m height. At position E5, the local exhaust is at 2.0 m height and low-velocity unit was at 1.7 m height. With the enhanced effect of the general exhaust, a short-circuit flow [40] was formed at position E5 with a higher risk of cross-infection. Therefore, it is suggested not to situate a workstation near the general exhaust with the low-velocity unit at 1.7 m. This phenomenon also occurs with the perforated duct at 1.7 m height, where positions E4 and E5 were exposed to a slightly higher risk.

3.2. Dilution ratio and infection probability

Fig. 9 shows the average dilution ratio (Equation (3)) for the five suspectable persons after the exhaust concentration reached a steady state condition. With the perforated duct and the airflow rate of 61 l/s, the dilution ratio remains relatively consistent among the five

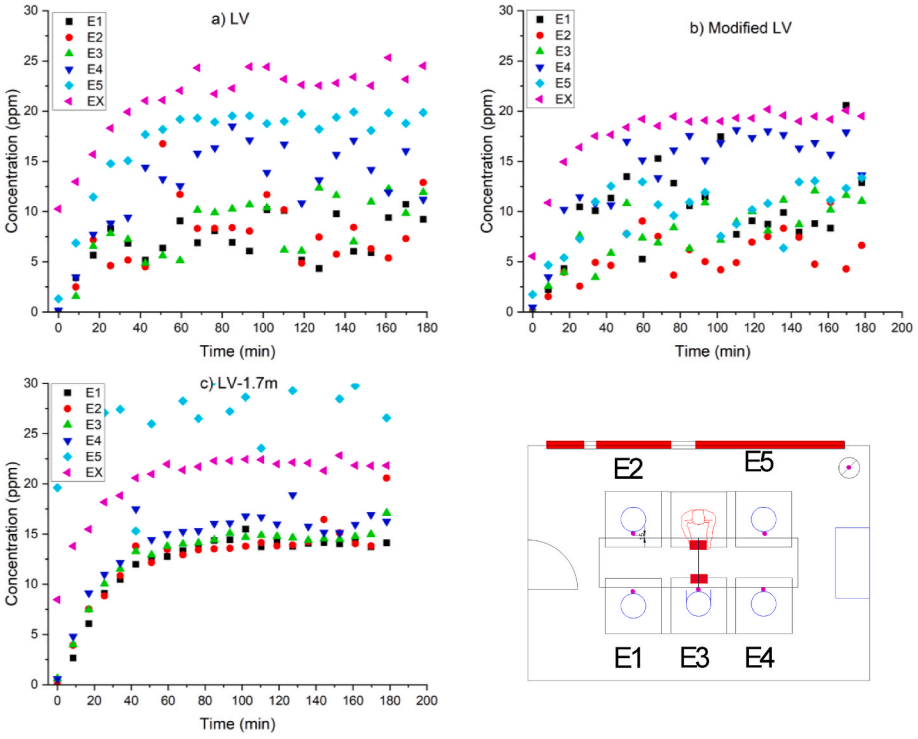

Fig. 7. Tracer gas distribution in the inhaled air of the five susceptible persons and general exhaust as a function of time with the heat gain of 36 W/m^2 and airflow rate of 61 l/s with the low-velocity unit located a) on the floor, b) an adjusted airflow pattern from the low-velocity unit with the perforated panel and c) attached to the wall at 1.7 m height.

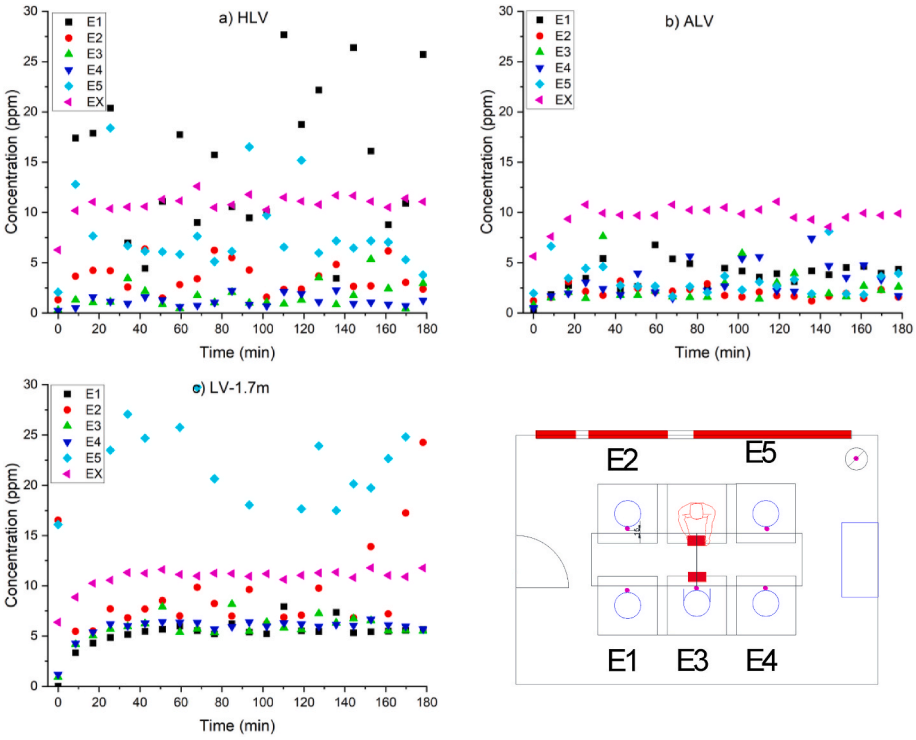

Fig. 8. Tracer gas distribution in the inhaled air of the five susceptible persons and general exhaust as a function of time with heat gain of 67 W/m^2 and airflow rate of 116 l/s with the low-velocity unit located a) on the floor, b) a modified air direction from the low-velocity unit with perforated panel and c) attached to the wall at 1.7 m height.

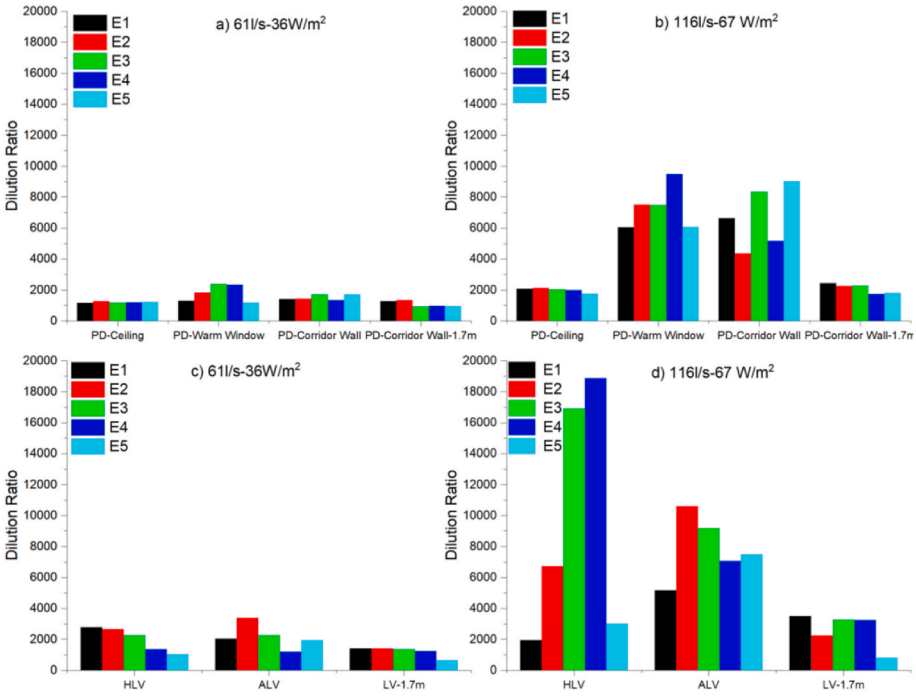

Fig. 9. Dilution ratio with for the five susceptible persons with the perforated duct and low-velocity unit systems.

suspectable persons. In comparison to the perforated duct in the ceiling and at 1.7 m height, the average values with the perforated duct on the floor was higher. Specifically, the average dilution ratios were 1821 and 1103 with the perforated duct under the warm window and at 1.7 m height, respectively. This means the average inhaled concentration was only 11.0 ppm while the exhaled concentration by the infector was 20000 ppm with the perforated duct under the warm window. Consequently, the dilution ratio increased by 40.4 % with the perforated duct under the warm window. With an airflow rate of 116 l/s, the corresponding values were 7333 and 2106 with the perforated duct under the warm window and at 1.7 m height, resulting in an increase of 71.2 %. As a result, the increasing airflow rate could improve the dilution ratio

greatly.

The dilution ratio under 61 l/s for the five suspectable persons was 2181 and 1230 with the adjusted low velocity unit and low velocity unit at 1.7 m height. With the airflow rate increasing to 116 l/s, the dilution ratio with the horizontally supplied low-velocity unit varied excessively between the five persons. Therefore, the horizontally supplied low velocity unit is not suitable for high airflow rate. With the low velocity unit at 1.7 m, the dilution ratio was 2627 and increased by 66.8 %–7910 with the adjusted low-velocity unit. The dilution ratio with the perforated duct under the warm window and adjusted low-velocity unit was quite similar at both airflow rates.

The human quanta yield varies based on pathogens and human activity. The quanta can be in the tens or hundreds when speaking. In these infection risk calculations, the yield of infected quanta has been assumed to be 5 quanta per hour [42], which is a moderate level. According to the Wells–Riley model which assumes that the indoor condition is fully-mixed and under steady-state conditions, the infection probability for all the susceptible persons varied between 2.4 % and 1.3 % with 61 l/s and 116 l/s after 3 h' exposure in the meeting room. Additionally, the infection probability varied with the locations of the susceptible persons, locations of the air terminal device and air distribution methods (Fig. 10).

In general, the infection probability with the perforated duct was much lower than in the fully mixed conditions. Especially when the perforated duct was located under the warm window and corridor wall on the floor, the cross infection was the lowest among the occupants. Combined with a local exhaust, the supply air rose to the breathing zone and the contaminant was effectively removed by the local exhaust efficiently. This phenomenon was more noticeable with the higher airflow rate where the higher local exhaust flow rate was used. The mean infection probability after 3 h' exposure was 0.9 % with an airflow rate of 61 l/s and reduced to 0.3 % with 116 l/s when the perforated duct was on the floor, as marked with the red circles.

With the low-velocity unit under the low airflow rate, the infection probability was lower than 2.4 %. However, position E5 (near the infector and general exhaust) exposed to a higher risk with the airflow rate of 116 l/s when the low-velocity unit was at 1.7 m height. When the airflow increased with the horizontally supplied low-velocity unit on the floor, the infection risk for position E1 (near the door and far from the diffuser) increased from 0.5 % to 1.1 %. Therefore, a higher airflow rate did not necessarily mean safer conditions with the low-velocity unit. The adjusted low-velocity unit showed the best performance concerning cross-infection. The supplied airflow at the floor level was delivered to the two sides of the meeting table where the occupants were seated. With the interaction between the thermal plume of the occupants and other heat gains, the cold air went up to the breathing zone to dilute the contaminant. The mean infection probability was 0.7 % with 61 l/s and 0.2 % with 116 l/s after 3 h' exposure.

3.3. Contaminant removal effectiveness (CRE)

In the fully mixed situation, the concentration in the exhaust is the same as in the whole room, which gives a CRE value equal to 1. In this study with the perforated duct on the ceiling and located at 1.7 m height, the CRE was quite uniform among the five susceptible persons (standard deviation (SD) = 0.1) and the average value was 1.1–1.3 (Table 4). When the perforated duct was under the warm window and corridor wall on the floor, the CRE value varied slightly, and it was 2.0 and 1.6 with the warm window and corridor wall, respectively. When the airflow rate increased to 116 l/s and the heat gain to 67 W/m^2, the CRE

Table 4
The contaminant removal effectiveness with different installation locations of perforated duct and low-velocity unit.

	36 W/m^2		67 W/m^2	
	Mean	SD	Mean	SD
PD-Ceiling	1.3	0.1	1.1	0.1
PD-Warm Window	2.0	0.6	4.3	1.1
PD-Corridor Wall	1.6	0.4	3.3	1.2
PD-Corridor Wall-1.7 m	1.1	0.0	1.1	0.1
HLV	2.3	0.6	5.3	2.8
ALV	2.1	0.5	3.9	1.3
LV-1.7 m	1.3	0.1	1.5	0.2

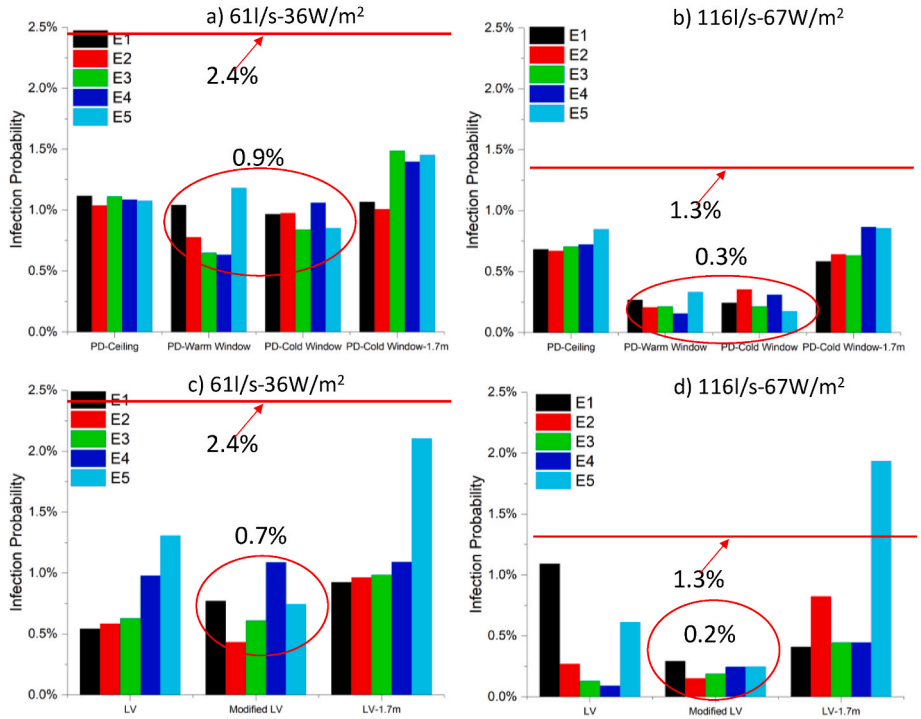

Fig. 10. Infection probability for the five susceptible persons with the perforated duct and low-velocity unit systems after 3 h' exposure time.

value was more uniform (SD = 0) with the perforated duct in the middle of the ceiling but decreased slightly. The increasing airflow had no effect on the air change efficiency. Therefore, it is more important to focus on the air distribution. Similarly to the perforated duct in the middle of the ceiling, the CRE value was quite stable when the perforated duct was at 1.7 m height.

If the perforated duct was located under the warm window and below the corridor wall, the CRE value fluctuated and the mean value was 4.3 and 3.3 with the perforated duct under the warm window and below the corridor wall, respectively. A possible reason for this is the combination effect of higher local airflow rate (10 l/s per person) from the local exhaust and higher supply airflow rate. In addition to this, the supply airflow from the floor level did not disturb the airflow to the local exhaust, which enhanced the contaminant removal. With an airflow rate of 61 l/s, the SD (0.6) was much higher with the perforated duct on the floor and increased to 1.2 with an airflow rate of 116 l/s. Therefore, the airflow pattern fluctuated but the CRE was higher when the perforated duct was on the floor.

Compared with the high-level installation, the low-level installation of the perforated duct worked better with both airflow rates studied. Especially, when the perforated duct was located under the warm window, the CRE value was higher than with the perforated duct under the corridor wall. One possible reason for this is that the airflow follows the thermal plume of the window and then turns down at the corridor wall and creates large eddies in the room space. But when the perforated duct was under the corridor wall, the airflow spread out over the floor and then drifted up the warm window side.

When the low-velocity unit was located on the floor (both horizontally supplied low-velocity unit and low-velocity unit with the adjusted air distribution) with 36 W/m^2 and 61 l/s, the SD of the CRE was large and showed high efficiency. The CRE with the low-velocity unit at 1.7 m was much lower but remained constant and did not vary during the measurement. The CRE with the low-velocity unit at 1.7 m was much lower and did not increase much when the airflow rate rose from 61 l/s to 116 l/s. When the airflow rate increased to 116 l/s and the heat gain increased to 67 W/m^2, the CRE fluctuated more with the low-velocity unit on the floor than that with the airflow rate of 61 l/s.

With the adjusted airflow pattern from the low-velocity unit, the CRE increased from 2.1 to 3.9 when the airflow rate was increased from 61 l/s to 116 l/s. This means the supply air can be delivered to every susceptible person with the adjusted low-velocity unit. However, the horizontally supplied low-velocity unit with an airflow rate of 116 l/s created an unstable airflow pattern, and the SD of the CRE reached to 2.8. This means the exposure level for every susceptible person varied greatly. Therefore, the horizontally supplied low-velocity unit is not a suitable solution in a small meeting room, when the specific airflow rate per unit is high as it could create eddies at the opposite wall. A better solution is to adjust the airflow pattern from the low velocity unit and then reduce the effect of the colliding flow on the opposite wall.

Overall, when perforated duct was located in the middle of the ceiling or attached to the corridor wall at 1.7 m and the low velocity unit at 1.7 m, the air distribution was closer to the mixing ventilation. The airflow pattern was quite stable in the room and the CRE value was approximately 1. When the perforated duct was under the warm window or corridor wall and the low velocity unit was on the floor with horizontal flow or adjusted flow pattern, the air distribution in the room was closer to the displacement ventilation. The airflow pattern slightly fluctuated and the CRE value was between 1.6 and 2.1 with an airflow rate of 61 l/s and double with the airflow rate of 116 l/s.

In the study, it was noticed that the airborne cross-infection was significantly lower when utilizing a more uniform distributed displacement airflow pattern, such as having a perforated duct on the floor and an adjusted airflow from a low-velocity unit on the floor. Therefore, during the design phase of ventilation systems, careful consideration of the placement of air diffusers together with location of exhaust points is crucial to minimize the risk of airborne transmission [43].

3.4. Experimental uncertainty

The total uncertainty is comprised random and systematic uncertainty in the measurements. The random uncertainty U_R is caused by random errors. Random errors are statistical fluctuations in the measured data. The random uncertainty can be reduced by taking more samples. The random uncertainty is given by

$$U_{R*} = \sqrt{\frac{\sum (x - \overline{x})^2}{(n-1) \times n}} = \frac{SD}{\sqrt{n}} \tag{8}$$

where U_{R*} is the random uncertainty (−), x is the single measurement, $\overline{x}$ is the average the of measurements, n is the number of measurements, and SD is the standard deviation. The percentage value of the random uncertainty U_R can be calculated as

$$U_R = \frac{U_{R*}}{\overline{x}} \times 100\% \tag{9}$$

The systematic uncertainty U_S is related to systematic errors. Systematic errors are reproducible inaccuracies due to aspects such as instrument errors. The systematic uncertainty of the equipment was 0.08 %. Finally, the total uncertainty U_T, based on both above mentioned parameters, is given by

$$U_T = \sqrt{{U_R}^2 + {U_S}^2} \tag{10}$$

In this study, the total uncertainty was defined for all obtained results of the tracer gas concentration. Based on Equations (8)–(10), the total uncertainty was in the range of 0.3 %–16.4 %, corresponding to the range of 0 ppm–1.7 ppm.

4. Discussion

The placement of supply and exhaust units can play a crucial role in mitigating infection risks in indoor environments. The study emphasizes the importance of air distribution solutions that are easy to implement and modify to create localized micro-environments around occupants. It contributes the idea that air distribution plays a significant role in determining local contaminant concentrations, especially when air terminal devices are positioned at floor level and the exhaust is near the occupants. Thus, a careful evaluation of the ventilation configuration can help in gaining insight and optimizing the flow path of air to obtain the desired combination of energy saving and the reduced risk of airborne transmission. This comprehensive approach not only ensures a high perception of indoor air quality but also contributes to creating healthier and safer environments for occupants.

It is crucial to assess the possible locations of vulnerable individuals within a room, recognizing that the level of risk can vary significantly in different locations [6]. However, it is challenging to estimate the exact location of person indoors. Consequently, providing instructions on seating arrangements when rooms are not fully occupied during a pandemic becomes crucial. Additionally, implementing sensors to monitor individual locations could inform ventilation system adjustments in real-time, enhancing the overall air quality management. By designing ventilation systems that accommodate individual positioning and airflow dynamics, it becomes possible to mitigate risks effectively and enhance indoor air quality.

With the low-velocity unit, it was observed that horizontally supplied air passing under the meeting table caused fluctuations in the airflow pattern. The highest SD of tracer gas distribution can reach 7.5 ppm with the low-velocity unit on the floor but only 1.7 ppm with modified low-velocity unit. To ensure optimal air distribution benefiting all occupants, it is essential that the airflow is evenly dispersed. A horizontal airflow from the low-velocity unit may not be ideal for this meeting room, as it can result in significant variations in pollutant exposure levels. To avoid the formation of eddies, the airflow from the

low-velocity unit should be directed and diffused effectively.

Increasing the ventilation airflow rate typically helps dilute particle concentrations and lower the average concentration levels within a space. However, it is important to note that raising the airflow rate under certain circumstances can lead in some conditions to higher local concentration levels compared to lower airflow rates [44]. It is important to recognize that solely raising the airflow rate does not always ensure improved ventilation effectiveness. Therefore, a comprehensive assessment of airflow patterns and distribution strategies is vital to optimize indoor air quality without inadvertently creating localized areas of higher pollutant concentrations.

In enclosed and mechanically ventilated rooms such as isolation rooms, the key factor in influencing contaminant transmission and control is the path from the contaminant source to the exhaust system. Contaminants are more effectively managed when this path remains uninterrupted by air streams, allowing for the efficient removal of the contaminants. Designing ventilation systems to create a direct, unobstructed path from the source to the exhaust enhances contaminant control in these environments. A combination of locations and type of supply diffusers, locations of the room exhaust and supply airflow rates can affect the airflow patterns, which are intricate and unique to each design configuration. This study indicates an overhead local exhaust combined with a proper supply air distribution establishes a ready flow path for airborne particles to exit the room without significant recirculation. However, determining the optimized design configuration and placement of supply diffusers and the exhaust in enclosed and mechanically ventilated rooms can be challenging due to variations in room layouts, airflow patterns, and specific contaminant sources. Factors such as the room size, layout, occupancy, and the size of contaminants play significant roles in deciding the most effective ventilation design. Careful evaluation of these factors is essential for achieving effective contaminant control and maintaining a healthy indoor environment.

This study focuses on airborne transmission with a tracer gas under steady state condition (no person walking). Therefore, this study cannot represent the transient airborne transmission under dynamic conditions. For example, the walking person disturbed the displacement principle and resulted in a decrease of the inhaled air quality with the displacement ventilation [45]. The influence of a moving manikin on mixing ventilation was less than for displacement ventilation. Moreover, the tracer gas SF_6 used in this study cannot simulate the complicated dynamic processes of exhaled aerosols, such as evaporation, condensation, coagulation, resuspension, and phase change. Additionally, the breathing process of the exposed person was not considered in this study. Finally, the parameters of breathing are varied due to age, gender, and metabolic rate, etc., which may also have some effect on the infection risk. Finally, the reliance on a singular chamber configuration experiment might not fully represent the complexity of real-world scenarios, such as diverse room geometries and conditions. Future research will address these limitations.

5. Conclusions

This study demonstrates that the supply airflow paths, airflow rate, local exhaust and supply units' location can work collaboratively to establish protective and effective contaminant control. In the present study, the performance of two types of air diffusers: perforated duct and low-velocity unit combined with local exhausts on airborne transmission and cross infection was investigated in a meeting room. The conclusions were as follows:

- Combined with a local exhaust, the concentration distribution in inhaled air was much lower with the perforated duct on the floor than on the ceiling and at 1.7 m height attached to a cold window. The performance of the perforated duct on the floor to mitigate airborne transmission is much better than that installed on the ceiling with higher a heat gain and airflow rate.
- Combined with the local exhaust, the concentration in the inhaled air varied with the low-velocity unit on the floor but was much more stable with the low-velocity unit at 1.7 m attached to the wall. With an adjusted air direction from the low-velocity unit, the inhaled concentration was much lower and uniform among the five susceptible persons.
- The CRE value was quite stable and slightly higher than the one when the perforated duct was located on the ceiling and at 1.7 m height. With the perforated duct on the floor, the CRE varied and increased with the airflow rate. The CRE value was 4.3 with the perforated duct attached to the warm window on the floor.
- A higher airflow rate led to a higher fluctuation of CRE when the low-velocity unit was on the floor. With the modified air direction from the low-velocity unit, the CRE was much more stable and increased from 2.1 to 3.9 when the airflow rate was from 61 l/s to 116 l/s.
- The dilution ratio with the perforated duct under the warm window and modified low-velocity unit was the highest.
- The infection probability with the perforated duct was much lower than in fully mixed conditions. This was especially the case when the perforated duct was attached to the warm window and corridor wall on the floor. The mean infection probability after 3 h' exposure was 0.9 % with an airflow rate of 61 l/s and reduced to 0.3 % with 116 l/s when the perforated was located on the floor.
- The higher airflow rate did not mean safer conditions with a low-velocity unit. The perforated duct on the floor and modified low-velocity unit showed the best performance for cross-infection.

Nomenclature	
PD	Perforated duct
LV	Low-velocity unit
PD Ceiling	Perforated duct in the middle of the ceiling
PD Warm Window	Perforated duct under the warm window on the floor
PD Corridor Wall	Perforated duct under the corridor wall on the floor
PD Corridor Wall-1.7 m	Perforated duct attached to the corridor wall at 1.7 m height
HLV	Low-velocity unit on the floor with horizontally supplied flow
ALV	Adjusted air pattern from low-velocity unit with perforated panels
LV 1.7 m	Low-velocity unit attached to the wall at 1.7 m height
CRE	Contaminant removal effectiveness
SD	Standard deviation

CRediT authorship contribution statement

Weixin Zhao: Writing – original draft, Methodology, Investigation, Formal analysis, Data curation, Conceptualization. **Muhammad Farhan Ejaz:** Writing – review & editing, Methodology. **Simo Kilpeläinen:** Writing – review & editing, Methodology, Conceptualization. **Juha Jokisalo:** Writing – review & editing. **Risto Kosonen:** Writing – review & editing, Supervision, Project administration, Funding acquisition, Conceptualization.

Declaration of competing interest

The authors declare that they have no known competing financial interests or personal relationships that could have appeared to influence the work reported in this paper.

Data availability

Data will be made available on request.

Acknowledgment

The study was supported by SUOJAILMA project funded by the Finnish Work Environment Fund (Grant No. 210099). HEATCLIM (Heat and health in the changing climate, Grant Numbers. 329306, 329307) funded by the Academy of Finland within the CLIHE (Climate change and health) Programme.

References

[1] L. Morawska, J.W. Tang, W. Bahnfleth, P.M. Bluyssen, A. Boerstra, G. Buonanno, J. Cao, S. Dancer, A. Floto, F. Franchimon, How can airborne transmission of COVID-19 indoors be minimised? Environ. Int. 142 (2020) 105832.
[2] L. Morawska, J. Cao, Airborne transmission of SARS-CoV-2: the world should face the reality, Environ. Int. 139 (2020) 105730.
[3] H. Qian, X. Zheng, Ventilation control for airborne transmission of human exhaled bio-aerosols in buildings, J. Thorac. Dis. 10 (2018) S2295.
[4] G.A. Somsen, C. van Rijn, S. Kooij, R.A. Bem, D. Bonn, Small droplet aerosols in poorly ventilated spaces and SARS-CoV-2 transmission, Lancet Respir. Med. 8 (2020) 658–659.
[5] H. Dai, B. Zhao, Association of the infection probability of COVID-19 with ventilation rates in confined spaces, in: Building Simulation, Springer, 2020, pp. 1321–1327.
[6] W. Zhao, S. Lestinen, M. Guo, S. Kilpeläinen, J. Jokisalo, R. Kosonen, An experimental study on airborne transmission in a meeting room with different air distribution methods, Build. Environ. (2024) 111522.
[7] W. Zhao, S. Lestinen, S. Kilpeläinen, X. Yuan, J. Jokisalo, R. Kosonen, M. Guo, Exploring the potential to mitigate airborne transmission risks with convective and radiant cooling systems in an office, Build. Environ. 245 (2023) 110936, https://doi.org/10.1016/j.buildenv.2023.110936.
[8] F. Liu, L. Zhang, H. Qian, The penetration phenomenon of the expiratory airflow from thermal plume of human body in the microenvironment around people, Build. Environ. 259 (2024) 111656, https://doi.org/10.1016/j.buildenv.2024.111656.
[9] A.K. Melikov, Human body micro-environment: the benefits of controlling airflow interaction, Build. Environ. 91 (2015) 70–77.
[10] Z.D. Bolashikov, A.K. Melikov, W. Kierat, Z. Popio\lek, M. Brand, Exposure of health care workers and occupants to coughed airborne pathogens in a double-bed hospital patient room with overhead mixing ventilation, HVAC R Res. 18 (2012) 602–615.
[11] W. Su, B. Yang, A. Melikov, C. Liang, Y. Lu, F. Wang, A. Li, Z. Lin, X. Li, G. Cao, Infection probability under different air distribution patterns, Build. Environ. (2021) 108555.
[12] L. Borro, L. Mazzei, M. Raponi, P. Piscitelli, A. Miani, A. Secinaro, The role of air conditioning in the diffusion of Sars-CoV-2 in indoor environments: a first computational fluid dynamic model, based on investigations performed at the Vatican State Children's hospital, Environ. Res. 193 (2021) 110343.
[13] Y. Song, C. Yang, H. Li, H. Chen, S. Shen, Y. Hou, J. Wang, Aerodynamic performance of a ventilation system for droplet control by coughing in a hospital isolation ward, Environ. Sci. Pollut. Res. 30 (2023) 73812–73824, https://doi.org/10.1007/s11356-023-27614-w.
[14] X. Kong, C. Guo, Z. Lin, S. Duan, J. He, Y. Ren, J. Ren, Experimental study on the control effect of different ventilation systems on fine particles in a simulated hospital ward, Sustain. Cities Soc. 73 (2021) 103102.
[15] I. Olmedo, J.L. Sánchez-Jiménez, F. Peci, M. Ruiz de Adana, Personal exposure to exhaled contaminants in the near environment of a patient using a personalized exhaust system, Build. Environ. 223 (2022) 109497, https://doi.org/10.1016/j.buildenv.2022.109497.
[16] T. Lee, J.-C. Soo, R.F. LeBouf, D. Burns, D. Schwegler-Berry, M. Kashon, J. Bowers, M. Harper, Surgical smoke control with local exhaust ventilation: experimental study, J. Occup. Environ. Hyg. 15 (2018) 341–350, https://doi.org/10.1080/15459624.2017.1422082.
[17] M.J. Jafari, A. Karimi, M.R. Azari, The role of exhaust ventilation systems in reducing occupational exposure to organic solvents in a paint manufacturing factory, Indian J. Occup. Environ. Med. 12 (2008) 82.
[18] Z. Cao, C. Zhai, Y. Wang, T. Zhao, H. Wang, Flow characteristics and pollutant removal effectiveness of multi-vortex ventilation in high pollution emission industrial plant with large aspect ratio, Sustain. Cities Soc. 54 (2020) 101990.
[19] A.B. Ngali, N. Mustaffa, Experimental investigation of local exhaust ventilation effectiveness at welding laboratory, Progress in Engineering Application and Technology 4 (2023) 563–571.
[20] Y.S. Eom, D.H. Kang, D. Rim, M. Yeo, Particle dispersion and removal associated with kitchen range hood and whole house ventilation system, Build. Environ. 230 (2023) 109986, https://doi.org/10.1016/j.buildenv.2023.109986.
[21] S. Nateghi, J. Kaczmarczyk, Compatibility of integrated physical barriers and personal exhaust ventilation with air distribution systems to mitigate airborne infection risk, Sustain. Cities Soc. 103 (2024) 105282, https://doi.org/10.1016/j.scs.2024.105282.
[22] E. Katramiz, N. Ghaddar, K. Ghali, Novel personalized chair-ventilation design integrated with displacement ventilation for cross-contamination mitigation in classrooms, Build. Environ. 213 (2022) 108885, https://doi.org/10.1016/j.buildenv.2022.108885.
[23] J. Yang, C. Sekhar, D.K. Cheong, B. Raphael, A time-based analysis of the personalized exhaust system for airborne infection control in healthcare settings, Science and Technology for the Built Environment 21 (2015) 172–178.
[24] K. Khankari, Role of HVAC system configuration on probable flow path of airborne pathogens in a patient room, Build. Eng. 119 (2013).
[25] S. Aghniaey, J.G. Williams, S.D. Chaitow, L. Rivera, Investigating air distribution designs for DOAS systems to reduce cross-contamination in open offices, Build. Eng. 127 (2021).
[26] Y. Liu, L. Bao, H. Wang, A. Yu, C. Ge, Reduced-scale experimental investigation on flow field characteristics of exhaust hood of double helix lifting transportation equipment in an industrial plant, Case Stud. Therm. Eng. 43 (2023) 102798.
[27] O.N. Zaitsev, K.I. Logachev, A.B. Gol'tsov, Increasing the pollutants capture rate by local exhaust due to the use of external swirling jet. Part 1. Research methods, Refract. Ind. Ceram. 63 (2022) 332–336, https://doi.org/10.1007/s11148-022-00731-8.
[28] O.N. Zaytsev, N.V. Tsopa, N.A. Stepancova, Processes of precession and nutation in swirling interacting gas jets, in: IOP Conference Series: Materials Science and Engineering, IOP Publishing, 2018 032053. https://iopscience.iop.org/article/10.1088/1757-899X/463/3/032053/meta. (Accessed 13 November 2023).
[29] C. Qin, Y. He, J. Li, W.-Z. Lu, Mitigation of breathing contaminants: exhaust location optimization for indoor space with impinging jet ventilation supply, J. Build. Eng. 69 (2023) 106250.
[30] H. Qian, Y. Li, P.V. Nielsen, C.-E. Hyldgaard, T.W. Wong, A.T. Chwang, Dispersion of exhaled droplet nuclei in a two-bed hospital ward with three different ventilation systems, Indoor Air 16 (2006) 111–128.
[31] M.F. Ejaz, S. Kilpeläinen, P. Mustakallio, W. Zhao, R. Kosonen, An experimental study on the efficacy of local exhaust systems for the mitigation of exhaled contaminants in a meeting room, Buildings 14 (2024) 1272.
[32] D. Zukowska, A. Melikov, Z. Popiolek, Impact of geometry of a sedentary occupant simulator on the generated thermal plume: experimental investigation, in: HVAC and R Research, 2012, pp. 795–811, https://doi.org/10.1080/10789669.2012.672925.
[33] P. Mustakallio, R. Kosonen, A. Korinkova, Full-scale test and CFD-simulation of radiant panel integrated with exposed chilled beam in heating mode, Build. Simulat. 10 (2017) 75–85, https://doi.org/10.1007/s12273-016-0309-0.
[34] P. Mustakallio, R. Kosonen, A. Melikov, The effects of mixing air distribution and heat load arrangement on the performance of ceiling radiant panels under cooling mode of operation, Science and Technology for the Built Environment (2017), https://doi.org/10.1080/23744731.2016.1262662.
[35] Vsr - nozzle channel. https://www.lindab.fi. (Accessed 24 August 2024).
[36] Halton zen ZRE - displacement ventilation unit, halton. https://www.halton.com/products/zre-en_gb/. (Accessed 23 August 2024).
[37] A. Li, Attachment Ventilation Theory, Springer Nature, 2023. https://library.oapen.org/handle/20.500.12657/63030.
[38] A. Melikov, J. Kaczmarczyk, Measurement and prediction of indoor air quality using a breathing thermal manikin, Indoor Air 17 (2007) 50–59.
[39] S. Zhang, Z. Lin, Dilution-based evaluation of airborne infection risk-Thorough expansion of Wells-Riley model, Build. Environ. 194 (2021) 107674.
[40] M. Mundt, H.M. Mathisen, M. Moser, P.V. Nielsen, Ventilation Effectiveness: Rehva Guidebooks, 2004.
[41] E.C. Riley, G. Murphy, R.L. Riley, Airborne spread of measles in a suburban elementary school, Am. J. Epidemiol. 107 (1978) 421–432.
[42] R. Covid, Guidance Document, How to Operate and Use Building Services in Order to Prevent the Spread of the Coronavirus Disease (COVID-19) Virus (SARS-CoV-2) in Workplaces, 2020.
[43] W. Zhao, P. Mustakallio, S. Lestinen, S. Kilpeläinen, J. Jokisalo, R. Kosonen, Numerical and experimental study on the indoor climate in a classroom with mixing and displacement air distribution methods, Buildings 12 (2022) 1314.
[44] F. Memarzadeh, W. Xu, Role of air changes per hour (ACH) in possible transmission of airborne infections, Build. Simulat. 5 (2012) 15–28, https://doi.org/10.1007/s12273-011-0053-4.
[45] H. Matsumoto, Y. Ohba, The influence of a moving object on air distribution in displacement ventilated rooms, J. Asian Architect. Build Eng. (2004), https://doi.org/10.3130/jaabe.3.71.